The cerebro-spinal fluid as a Biomechanical marker in SCI

Laboratory of Applied Biomechanics
Aix-Marseille Université - Université Gustave Eiffel
Morgane EVIN

8^{th} of June, 2023

Laboratoire de
Biomécanique
Appliquée
UMR T24 IFSTTAR AMU

Spine Biomechanics

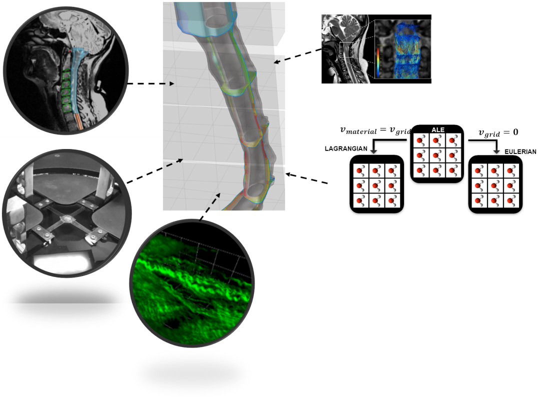

Context: Biomechanical role of the cerebro-spinal fluid

Spinal cord injury (SCI)

250,000 and 500,000 injuries: 10.5 new/100.000 pers/year *Kumar et al., 2018*

Societal issue

Associated cost:
0.1-2.19 million € (UK, Spain)
33 % tetraplegia, paraplegia
Pronostic marker, quality of life

Decompression surgery

To restore CSF pulsation or SC decompression

Mechanisms associated to SCI

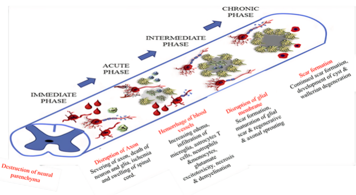

Anjum et al., 2020

Treatements of SCI

Stem cells, Electrostimulation, early mobilisation

SCI fact 2016, World Health Organisation, Witiw et Fehlings, 2015

Cerebro spinal fluid (CSF)

Cerebro spinal fluid (CSF)

- Newtonian Fluid
- Pulsation indexed on cardiac cycle
- Components of the SC canal

Rational for CSF Biomechanical role in SCI

CSF Biomarker - primary or cellular cascades
ASIA Score : 89% Prediction in 72h post injury

Hypothesis: The CSF has a role in the restoration or alteration of the SCI patients.

Question: How to create a CSF biomechanical marker at the patient's bedside?

Morphology of the subarachnoidal canal

Cervical Subarachnoidal Canal

11 Healthy volunteers - T2-Space
Supine and Flexion - *Sudres et al., Spine, 2021*

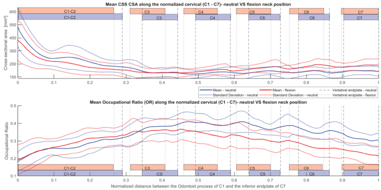

TABLE 4. Summary Table of the Main Results for Each Index

Morphological Parameters	Main Position-dependent Evolution
CSS CSA	Significant decrease from C1 to C3 superior endplate. From C3 to C7, low variation and oscillating phase around 157 mm^2 in neutral and 162 mm^2 in flexion positions.
SC CSA	Significantly lower in flexion than in neutral supine position.
OR	After the superior C3 endplate (0.33–neutral; 0.35–flexion), the flexion OR decreases faster than in neutral position.
CR	The CR index decreased steadily between C2 dens and to C7 inferior endplate for both posture. The CR for the flexion case is systematically lower.
AP eccentricity index	Same location for the both postures before C3 vertebra. After C3, in flexion the SC is more anteriorly positioned with respect to the center of the canal.
LR eccentricity index	Spinal cord centered (shift of 3% from the center of the canal) in the canal for the both postures.
Characteristics lengths	Significantly different in neck flexion than in neutral supine position (+2, 13, and 18 mm for the anterior column [LAC], posterior column [LPC], and spinal cord, respectively).

AP indicates antero-posterior; CR, compression ratio; CSS, cervical subarachnoid space; LAC, length of the anterior column; LPC, length of the posterior column; LR, Left–Right; OR, occupational ratio; SC, spinal cord.

Findings

- Poisson effect - Spinal cord morphology change
- Normal ranges and 3D characterization

Next to be published:

- Degenerative Cervical Myelopathy. Frebourg et al., 2021. *Sudres et al.*
- Traumatic Spinal Cord Injury. Berriot et al., CMBBE. *Berriot et al.*

PhD Student **P. Sudres, 2021**

Collaboration CRMBM, V. Callot.

Meningeal tissues characterization - Uniaxial

Meninges - literature

Uniaxial characterization - Tensile mostly
DAC - Dura matter and Archnoïd complex
Differences between orientation and species

Uniaxial tensile test

Swine model
Pre-load 0.5 N and 2 N for the DAC
Preconditioning 30 cycles
Load 0.2 mm/s
Collaboration, ETS, Y. Petit

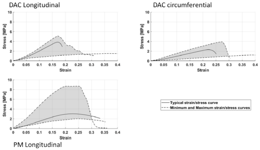

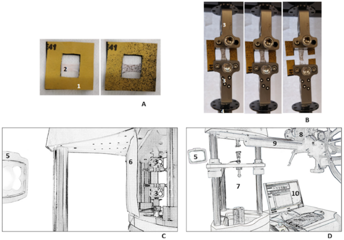

Results

Differences between spinal locations in DAC not in PM
Uncertainty measurements (Monte Carlos)

Preservation method: Flash frozen (ok

DAC - PM dft).

Sudres, Evin et al., 2021

Meningeal tissues characterization - Biaxial

Biaxial Methodology - literature

De Kegel et al., 2017, Shetye et al., 2014.

Biaxial tensile test System

Costumed made system

- 4 step motors Zaber and 4 load cells
- HBM/ National Instrument LabView program
- Pre-load 0.01N.
- 0.05 mm/s on 7mm .

Collaboration, CEMEF, Y. Tillier

Bi-photon microscopy - Collagen type II

Collaboration, INT

Constitutive models comparison

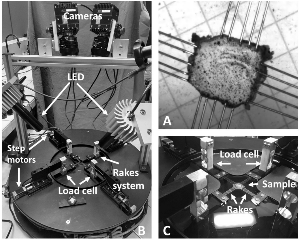

Quasi-static biaxial tensile test

Constitutive model and micro-structure

$$W_{Ani.GOH} = C_{10}(I_1 - 3) + C_{20}(I_1 - 3)^2 + \frac{k_1}{2k_2}[e^{k_2\{\kappa_1(I_1-3)+(I_1-3\kappa_1)(I_4-1)\}^2} - 1] + \frac{k_3}{2k_4}[e^{k_4\{\kappa_2(I_1-3)+(1-3\kappa_2)(I_6-1)\}^2} - 1]$$

Evin et al, 2022, Acta Biomat.

Constitutive modelling

Name	Nb of par.	Parameters	Model used for the matrix-based material W_{matrix}, number of fibers population	Ref.	Strain Energy function
Ogden	2	μ(MPa) β(-)	isotropic modified Ogden model (n=1)	[38]	$W_{fibres} = \frac{\mu}{\beta^2}[\lambda_{11}^{\beta} + \lambda_{22}^{\beta} + \lambda_{33}^{\beta} - 3]$
Reduced GOH	3	C_{10}(MPa) k_1(MPa) k_2(-)	matrix based NH model, and κ=1/3 (maximum dispersion), 1 fibers population	[32]	$W_{red\_GOH} = C_{10}(I_1 - 3) + \frac{k_1}{2k_2}[e^{k_2\{kI_1-1\}^2} - 1]$
Ani. GOH	5	C_{10}(MPa) k_1(MPa) k_2(-) κ(-) β(rad)	matrix based NH model, 1 fibers population	[32]	$W_{Ani.GOH} = C_{10}(I_1 - 3) + \frac{k_1}{2k_2}[e^{k_2\{\kappa I_1+(1-3\kappa)I_4-1\}^2} - 1 + e^{k_2\{\kappa I_1+(1-3\kappa)I_6-1\}^2} - 1]$
Trans. Iso Gasser	6	C_{10}(MPa) C_{20}(MPa) k_1(MPa) k_2(-) κ(-) β(rad)	matrix based Yeoh model, 1 fibers population	[14]	$W_{TIG} = C_{10}(I_1 - 3) + C_{20}(I_1 - 3)^2 + \sum_{i=4,6}\frac{k_1}{2k_2}[e^{k_2\{k(I_1-3)+(I_1-3k)(I_i-1)\}^2} - 1]$
Ani. Gasser	10	C_{10}(MPa) C_{20}(MPa) k_1(MPa) k_3(MPa) k_2(-) k_4(-) κ_1(-) κ_2(-) β(rad) γ(rad)	matrix based Yeoh model, 2 fibers populations	[14]	$W_{Ani.Gasser} = C_{10}(I_1 - 3) + C_{20}(I_1 - 3)^2 + \frac{k_1}{2k_2}[e^{k_2\{\kappa_1(I_1-3)+(I_1-3\kappa_1)(I_4-1)\}^2} - 1] + \frac{k_3}{2k_4}[e^{k_4\{\kappa_2(I_1-3)+(1-3\kappa_2)(I_6-1)\}^2} - 1]$
Mooney-Rivlin Fibers strengthening	6	C_{10}(MPa) C_{30}(MPa) k_1(MPa) k_2(-) κ(-) β(rad)		[38]	For $\lambda_d \leq 1$, $W_2 = 0$ For $1 < \lambda_d \leq \lambda_d^*$, $W_{21} = k_3(e^{-k_4(\lambda_d-1)} - 1)$ For $\lambda_d^* < \lambda_d$, $W_{22} = k_1\lambda_d + k_2$.

Optimization

Matlab function “lsqcurvefit”.

Trust region reflective algorithm.

DAC modeling

Mechanical Strain/stress

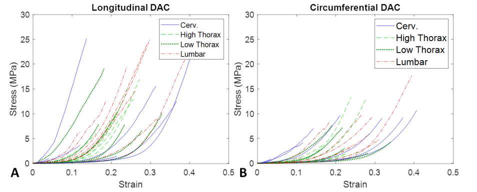

- 96.8 to 122.5 MPa vs 44.3 to 58.6 MPa
- Significant differences in thoracic and lombar DAC between orientations
- Transversely isotropic and anisotropic Gasser models (r^2=0.99 and RMSE:0.4 and 0.3 MPa)

Microscopy

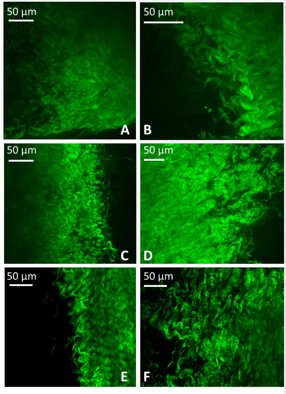

PM modeling

Mechanical Strain/stress

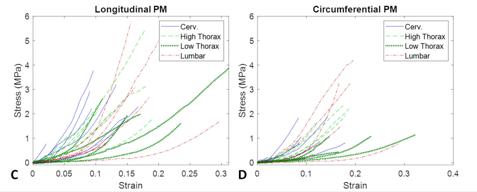

- 20.2 to 31.9 MPa vs 6.7 to 15.6 MPa
- Significant differences in cervical and thoracic PM between orientations
- Slightly significant difference between spinal level in circumferential thoracic PM
- Transversely isotropic and anisotropic Gasser models (r^2=1 and RMSE:0.06 and 0.07 MPa) modelling

Microscopy

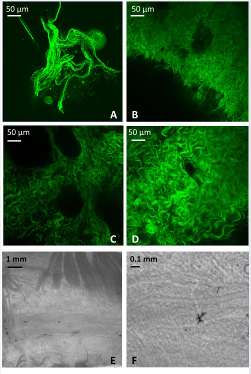

Meningeal tissues characterization - to be continued

Limitations of the previous study

Coefficient identification
unicity and initial parameter influence
Number of tested conditions

Protocol improvement

5 conditions (ratio 1:1, 1:2, 1:4, 2:1, 4:1)
Laville [...] Tillier, 2020
MOOPI Roux, Tillier et al. 2021

11 Macaque samples (PM and DAC)
6 conditions: 132 tests

De Kegel et al., 2017, Shetye et al., 2014.

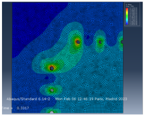

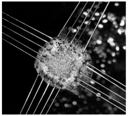

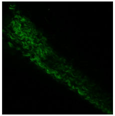

Preliminary results

Failure test analysis

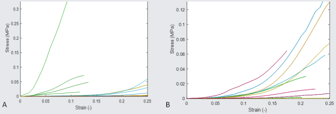

Nerves roots and ligaments characterization

PhD Student A. Berriot
Collaboration ETS, E. Wagnac.

Nerves roots and ligaments

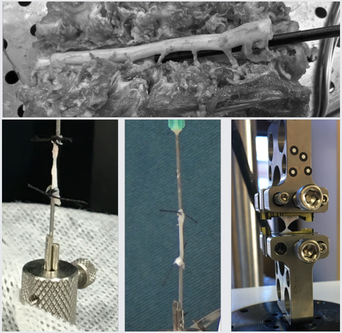

Singh et al, 2006, Tamura et al, 2017

Uniaxial characterization

- Mach-1 (Biomomentum, Montréal, Canada)
- 17N load Cell
- Bi-linear piece-wise fitting

Particularities

- Cervical spine and nerve types
- Ogden material model (1st to 3rd).

Submitted to JoB and continued (denticulae ligaments)

Cerebro-Spinal Fluid Numerical simulation

Master Internship Lugdivine Leblond

Meninges

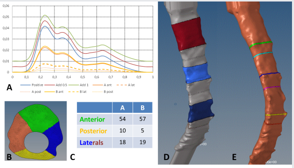

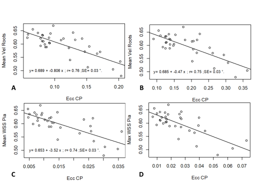

Cheng et al, 2017, Pahlavian et al, 2014

Simulations

- AcuSolve - Altair Suite
- Sensitivity analysis - 40y. old male
- Patient-specific morphology - 11 patients
- Boundary conditions - not MRI based

Taking into account Fluid-structure interaction

- Explicit vs Implicit solver
- Solver dependency
- Approach dependency

Of mice and men